AMERICAN JOURNAL OF PHYSIOLOGY
RENAL PHYSIOLOGY

Am J Physiol Renal Physiol 323: F81–F91, 2022.
First published May 2, 2022; doi:10.1152/ajprenal.00344.2021

RESEARCH ARTICLE

Inhibition of hypoxia-inducible factor-prolyl hydroxylation protects from cyclophosphamide-induced bladder injury and urinary dysfunction

Douglass B. Clayton,[1]* Ching Man Carmen Tong,[1] Belinda Li,[1] Abby S. Taylor,[1] Shuvro De,[1] Matthew D. Mason,[1] Anne G. Dudley,[1] Olena Davidoff,[2,3] Hanako Kobayashi,[2,3] and Volker H. Haase[2,3,4]*

[1]Division of Pediatric Urology, Department of Urology, Vanderbilt University Medical Center, Nashville, Tennessee; [2]Division of Nephrology and Hypertension, Department of Medicine, Vanderbilt University Medical Center, Nashville, Tennessee; [3]Medical and Research Services, Department of Veterans Affairs Hospital, Tennessee Valley Healthcare System, Nashville, Tennessee; and [4]Department of Molecular Physiology and Biophysics, Vanderbilt University School of Medicine, Nashville, Tennessee

Abstract

Disruption of the blood-urine barrier can result in acute or chronic inflammatory bladder injury. Activation of the oxygen-regulated hypoxia-inducible factor (HIF) pathway has been shown to protect mucosal membranes by increasing the expression of cytoprotective genes and by suppressing inflammation. The activity of HIF is controlled by prolyl hydroxylase domain (PHD) dioxygenases, which have been exploited as therapeutic targets for the treatment of anemia of chronic kidney disease. Here, we established a mouse model of acute cyclophosphamide (CYP)-induced blood-urine barrier disruption associated with inflammation and severe urinary dysfunction to investigate the HIF-PHD axis in inflammatory bladder injury. We found that systemic administration of dimethyloxalylglycine or molidustat, two small-molecule inhibitors of HIF-prolyl hydroxylases, profoundly mitigated CYP-induced bladder injury and inflammation as assessed by morphological analysis of transmural edema and urothelial integrity and by measuring tissue cytokine expression. Void spot analysis to examine bladder function quantitatively demonstrated that HIF-prolyl hydroxylase inhibitor administration normalized micturition patterns and protected against CYP-induced alteration of urinary frequency and micturition patterns. Our study highlights the therapeutic potential of HIF-activating small-molecule compounds for the prevention or therapy of bladder injury and urinary dysfunction due to blood-urine barrier disruption.

NEW & NOTEWORTHY Disruption of the blood-urine barrier can result in acute or chronic inflammatory bladder injury. Here, we demonstrate that pharmacological inhibition of hypoxia-inducible factor (HIF)-prolyl hydroxylation prevented bladder injury and protected from urinary dysfunction in a mouse model of cyclophosphamide-induced disruption of the blood-urine barrier. Our study highlights a potential role for HIF-activating small-molecule compounds in the prevention or therapy of bladder injury and urinary dysfunction and provides a rationale for future clinical studies.

cystitis; hypoxia-inducible factor; molidustat; prolyl hydroxylase domain dioxygenases; urinary dysfunction

INTRODUCTION

Disruption of the blood-urine barrier, the body's most impermeable barrier, results in bladder inflammation, i.e., cystitis, a highly prevalent urological condition, which affects millions of patients in the United States annually and significantly contributes to healthcare expenses (1–3). The causes of cystitis are broad and include infections, foreign bodies such as urinary stones and catheters, bladder outlet obstruction, and cellular injury from chemotherapy or pelvic radiotherapy. Over time, chronic cystitis can lead to fibrosis and loss of tissue compliance, which impairs bladder function. Ultimately, the loss of bladder compliance increases the hydrostatic pressure transmitted to the upper urinary tract causing damage to the renal parenchyma.

To improve urological care, patients need effective therapies that can dampen bladder inflammation and prevent chronic inflammation and long-term bladder damage. Currently, few targeted therapies exist for patients with chronic cystitis. For instance, in cases of severe hemorrhagic cystitis from chemotherapy, primary strategies are untargeted and include hyperhydration with intravenous fluids and administration of toxin-binding compounds like sodium-2-mercaptoethanesulfonate (MESNA) (4). In severe cases of radiation-induced cystitis in patients with oncology, treatment may be limited to the management of hematuria symptoms with agents instilled in the bladder such as formalin and 1% aluminum sulfate (5). These instillations can be painful and can require administration under general anesthesia. Furthermore, treatments such as formalin can defunctionalize the bladder due to fibrosis. Thus,

*D. B. Clayton and V. H. Haase contributed equally to this work.
Correspondence: V. H. Haase (volkerhhaase@gmail.com); D. B. Clayton (douglas.b.clayton@vumc.org).
Submitted 16 September 2021 / Revised 25 April 2022 / Accepted 25 April 2022

treatments that target the underlying bladder biology and pathophysiology are needed.

We have previously established that activation of hypoxic and/or hypoxia-inducible factor (HIF) signaling is associated with bladder injury secondary to partial outlet obstruction, a major cause of bladder dysfunction that begins with cystitis and progresses to bladder fibrosis (6). In line with these findings are gene expression data from single-cell analysis suggesting HIF pathway activation (7). Since the HIF pathway plays an important role in the control of mucosal barrier function and innate and humoral immune responses and promotes epithelial survival during periods of cellular stress (8–11), selective targeting of the HIF pathway has therapeutic potential for the prevention or treatment of different forms of bladder diseases.

The HIF pathway is highly conserved across eukaryotic organisms and is critical for cellular adaptation to hypoxic stress. HIF family members function as heterodimeric, activating transcription factors composed of a tightly oxygen-regulated α-subunit (either HIF-1α, HIF-2α, or HIF-3α) and a constitutively expressed nuclear β-subunit (HIF-β) (12). HIF activity is controlled by prolyl-4 hydroxylase domain enzymes (PHD1, PHD2, and PHD3), which belong to a larger family of 2-oxoglutarate-dependent dioxygenases that carry out various hydroxylation reactions (13). Under normoxic conditions, HIF-α proteins, which are continuously synthesized by cells, are rapidly degraded. PHDs use molecular oxygen and 2-oxoglutarate for the hydroxylation of specific proline residues within the oxygen-dependent degradation domain of HIF-α. Hydroxylation promotes binding to the von Hippel-Lindau-E3-ubiquitin ligase complex, which initiates the proteasomal degradation of HIF-α (14). Under hypoxic conditions, PHD catalytic activity is impaired due to reduced availability of molecular oxygen resulting in cellular HIF-α accumulation and nuclear translocation. In the nucleus, HIF-α dimerizes with HIF-β, forming a functional transcription factor that increases the expression of multiple oxygen-regulated genes (14).

Multiple studies have demonstrated that acute activation of HIF signaling by either genetic or pharmacological means is beneficial in organ injury and inflammation (10, 15–17). Pharmacological HIF activation can be accomplished by either oral or parenteral administration of structural analogs of 2-oxoglutarate, which inhibit PHD catalytic activity, thus preventing the degradation of HIF-α (18).

Here, we established a model of acute, cyclophosphamide (CYP)-induced disruption of the blood-urine barrier in mice to investigate the HIF-PHD axis in urothelial injury, bladder inflammation, and voiding dysfunction. For this, we used a pharmacological approach and studied the effects of two small-molecule HIF-prolyl hydroxylase inhibitors (HIF-PHIs): dimethyloxalylglycine (DMOG) and molidustat. DMOG is a frequently used tool compound for in vitro experiments and preclinical animal studies (19–22), whereas molidustat is a new oral, daily administered HIF-PHI, approved for clinical use in Japan (23–25). Our data demonstrate that pharmacological HIF activation mitigated CYP-induced bladder injury and voiding dysfunction and provide a rationale for future clinical studies to investigate HIF-PHIs as therapeutic agents in the prevention and therapy of urothelial injury and bladder inflammation due to blood-urine barrier disruption.

METHODS

Animals

Eight- to twelve-week-old male C57BL/6 mice were used for experiments (Charles River Laboratories, Wilmington, MA). Mice were fed standard chow and given free access to water except during the micturition assays. All procedures involving mice were performed per the National Institutes of Health guidelines for the use and care of live animals and were approved by the Vanderbilt University Institutional Animal Care and Use Committee.

Drug Administration

Mice received 37.5, 75, 150, or 300 mg/kg CYP by intraperitoneal injection (Sigma-Aldrich, St. Louis, MO). CYP solutions were prepared fresh with normal saline as a vehicle. DMOG (Cayman Chemical, Ann Arbor, MI) was administered in 100 μL of 0.9% saline intraperitoneally at a dose of 16 mg/injection immediately following CYP administration; vehicle controls received 100 μL saline. Molidustat (Bay 85-3934, Cayman Chemical) was dissolved in a vehicle consisting of 90% sunflower oil and 10% ethanol. Treatment groups received molidustat (10 mg/kg) or vehicle by oral gavage, given as a pretreatment at 48, 24, and 6 h before CYP administration.

Bladder Injury Assessment

Bladder injury was assessed by measuring bladder-to-body weight ratios (mg/g), by scoring histologic edema, and by assessing urothelial integrity. Bladders were sectioned and fixed in 10% neutral-buffered formalin followed by paraffin embedding. Tissue sections (3–5 μm) were stained with hematoxylin and eosin. Slides were digitally archived using whole slide imaging at ×20 magnification to a resolution of 0.5 μm/pixel using a Leica SCN400 Slide Scanner automated digital image system (Leica Biosystems, Wetzlar, Germany). High-resolution images were selected using Aperio ImageScope (Lecia Biosystems) and deconstructed to allow quantification of tissue areas for edema, detrusor muscle, and the urothelium based on pixel count using Photoshop CC 2019 (Adobe, San Jose, CA). Pixel counts in deconstructed images were calculated using FIJI ImageJ software (https://imagej.net/Fiji). Edema scores were calculated by dividing the total area of edema by the total tissue area. Urothelial integrity was calculated by dividing the total urothelial area by the total detrusor muscle area.

Micturition Assay

The void spot assay (VSA) permits the study of voiding behavior and void volume in mice (26). For all experiments, mice were individually acclimated to standard plastic mouse cages lined with Whatman grade 1 filter paper (Thermo Fisher Scientific, Waltham, MA) cut to cage bottom dimensions (14.9 cm × 29.5 cm) 1 day before CYP or vehicle administration. For VSAs, sections of filter paper were placed between cages to reduce the potential for stress-induced bladder phenotypes from visual contact with other mice. One piece of mouse chow was placed in each cage and water was not provided during VSAs. Cages were kept in a noise-free section of the laboratory space during testing. A separate study to assess

whether repeated VSAs induce stress voiding phenotypes was conducted over eight consecutive days followed by a 2-day break and then VSAs for two more consecutive days. For CYP injury experiments, mice were acclimated for 1 day and returned to the animal facility. VSAs of 4-h duration were performed at 2, 24, 48, and 72 h following CYP administration. VSA filter papers were analyzed after drying for 24 h. Voiding spots were visualized in a UVP EpiChemi II Darkroom cabinet with a 365-nm epi-illuminator and a clear overhead filter (Analytik Jena, Upland, CA). Images were captured with a Canon E6 camera and a Canon EF 35 mm f/1.4L II USM Lens (Canon Cameras, Tokyo, Japan) with settings refined for improved signal-to-noise ratio. VSA images were converted to tiff files and batch processed using the Void Whizzard plugin for FIJI ImageJ with a lower limit threshold of 0.01 cm^2, which corresponds to urine volumes of <0.2 μL, as previously described (27).

Bladder Permeability Assay

The permeability of the bladder was assessed as previously described (28). Twenty-four hours after drug exposure, mice were catheterized under anesthesia. The bladder was instilled with 30 μL of 0.4% (wt/vol) methylene blue (Sigma-Aldrich) dissolved in 0.9% saline. The methylene blue solution was left indwelling for 20 min, after which the bladder was rinsed with 1.5 mL sterile saline. Methylene blue retained in the bladder was extracted with chloroform (Sigma-Aldrich) at 45°C overnight and quantified spectrophotometrically at a wavelength of 660 nm (Thermo Fisher Scientific).

RNA Analysis

Bladders harvested for RNA analysis were immediately placed into RNAlater (Qiagen, Hilden, Germany). RNA was isolated using a column-based extraction method (RNAeasy, Qiagen), and samples were quantified with a Nanodrop 2000 spectrophotometer (Thermo Fisher Scientific). cDNA was prepared by reverse transcription (Iscript Reaction Mix, Bio-Rad, Hercules, CA), and gene expression was investigated by quantitative PCR using a CFX96 thermocycler platform and SYBR Green Master Mix (Bio-Rad, Hercules, CA). Relative gene expression was analyzed by the $2^{-\Delta\Delta Ct}$ method (where C_t is threshold cycle). Primer sequences used for the quantitative PCR analyses are provided in Supplemental Table S1 (all Supplemental Material is available at https://doi.org/10.6084/m9.figshare.16574267.v1).

Cytokine Measurements

Bladders were weighed, snap-frozen, and stored at −80°C until analysis. Before homogenization, samples were placed in RIPA buffer (20 mg bladder tissue/mL) containing 10 μL/mL Halt Protease Inhibitor (Thermo Fisher Scientific). After a quick mincing with scissors, samples were homogenized using an air-cooled Bullet Blender with Navy Tubes (Next Advance, Troy, NY) and stored at −20°C until analysis. IL-6, IL-1b, keratinocyte-derived chemokine/chemokine (C-X-C motif) ligand 1 (KC/CXCL1), monocyte chemoattractant protein-1/chemokine (C-C motif) ligand 2 (MCP-1/CCL2), macrophage inflammatory protein-2/chemokine (C-X-C motif) ligand 2 (MIP-2/CXCL2), and vascular endothelial growth factor (VEGF) were measured using the Milliplex Mouse Cytokine/Chemokine Panel (Millipore Sigma, Burlington, MA) on a Luminex MagPix System (Luminex, Austin, TX).

Serum Erythropoietin

Blood samples were obtained via cardiac puncture, and serum erythropoietin (EPO) levels were measured using the Mouse Erythropoietin Quantikine ELISA kit (R&D Systems, Minneapolis, MN) 6 h after the administration of DMOG or molidustat.

Immunohistochemistry

To assess urothelial cell proliferation, K_i-67 antigen was detected with rabbit monoclonal antibody (ab16667, Abcam, Cambridge, MA) in conjunction with goat anti-rabbit IgG secondary antibody (Vector Laboratories, Burlingham, CA). Ten random high-power fields per bladder section were examined for K_i-67-positive cells, and the percentage of positive urothelial cells was determined using the National Institutes of Health ImageJ software (rsbweb.nih.gov/ij). To assess HIF-1α staining, bladder and kidney sections were stained as previously described with polyclonal rabbit anti-HIF-1α antiserum (Cat. No. 10006421, Cayman Chemical) at a dilution of 1:10,000 (29). The CSA-II high signal amplification kit and Rabbit Link reagent (DAKO) were used for detection following the manufacturer's instructions.

Urinary *N*-Acetyl-*S*-3-Hydroxypropylcysteine Analysis

To assess urine acrolein levels, we measured acrolein metabolite *N*-acetyl-*S*-3-hydroxypropylcysteine (3-HPMA), which is formed from glutathione and acrolein (30). For this, mice were housed individually in standard metabolic cages for 6 h. Urine was collected hourly, and collections were pooled for the analysis. Samples were analyzed with liquid chromatography-tandem mass spectrometry (MS) by the Masonic Cancer Center Analytical Biochemistry Shared Resource at the University of Minnesota as previously described (31).

Blood Sampling and MS for CYP Metabolites

CYP is a prodrug and is rapidly converted in the liver to 4-hydroxycyclophosphamide (4-OH-CYP), which is the active metabolite, ultimately becoming phosphoramide mustard (32). Plasma levels of CYP and 4-OH-CYP were measured quantitatively in the MS Core Laboratory at Vanderbilt University Medical Center by reverse-phase liquid chromatography coupled with tandem MS detection using a stably labeled CYP-d_4 isotopologue (TRC) as the internal standard. For calibration of the instrument response, normal plasma was spiked with specified amounts of CYP, 4-hydroperoxy CYP (4-OOH-CYP), CYP-d_4, and an excess of sodium thiosulfate to generate unstable 4-OH-CYP via chemical reduction of the hydroperoxide. Samples and calibration standards were derivatized with dansyl hydrazine and extracted with methyl *tert*-butyl ether before liquid chromatography-MS analysis. The aldophosphamide tautomer of 4-OH-CYP was measured as its dansyl hydrazone derivative.

Statistical Analysis

Experimental numbers were determined by power calculations based on prior experience with multiple end points (*Il6* gene expression, histological scoring, and voiding frequency)

using a probability of 0.05 (α) for type I errors and 0.2 (β) for type II errors. Nonpaired Student's *t* tests were used for two-group comparisons, and one-way ANOVA followed by Dunnett's post hoc analysis or Bonferroni's correction, respectively, were used for multigroup comparisons (GraphPad Prism v.9.0, San Diego, CA). *P* values of <0.05 were considered statistically significant.

RESULTS

CYP Induces Rapid Bladder Injury and Alters Micturition Patterns in Mice

To establish a model of acute CYP-induced blood-urine barrier disruption in mice, we tested different CYP doses and found that a single intraperitoneal administration of 300 mg/kg resulted in robust and reproducible bladder injury. We investigated the time course of bladder injury development and recovery by examining bladder weight, permeability, bladder morphology, inflammatory gene expression, and cytokine levels in bladder tissue. Mice were analyzed at 6, 28, 52, and 76 h after intraperitoneal administration of 300 mg/kg CYP (Fig. 1*A*). Bladder-to-body weight ratios peaked at 28 h after CYP exposure (3.1-fold increase) with bladder weights declining by 76 h (1.6-fold) compared with vehicle-treated controls (Fig. 1*A*). Morphologically, CYP-induced injury was characterized by severe bladder wall edema, urothelial sloughing, and hemorrhage within the lamina propria and mucosa, which was associated with increased bladder permeability (Fig. 1*A* and Supplemental Fig. S1). Using a scoring method that assesses the area of tissue with edema and urothelial thickness in relation to the total tissue area and area covered by detrusor muscle, respectively, we found significantly increased bladder wall edema that peaked at 28 h (~21-fold increase) after CYP (Fig. 1*A*). The time course of bladder wall edema development and resolution followed bladder weight and urothelial integrity score (Fig. 1*A*). Inflammatory gene expression from whole bladder homogenates revealed a significant increase in *Il6* and *Il1b* transcript levels 28 h after CYP (Fig. 1*B*). Consistent with bladder inflammation was the increase in bladder cytokines IL-6, VEGFA, MCP-1/CXCL1, and MIP-2/CCL2 6 h after CYP exposure (Fig. 1*C*). In a separate experiment, we assessed animals for signs of organ injury beyond the bladder, as demonstrated in a prior study (33). Significant organ injury was not detected in kidney, liver, and heart tissue at 24 h following CYP administration by histological evaluation (Supplemental Fig. S2).

Prior to micturition assessments, all mice were specifically acclimated to the VSA 1 day before initiation of the experiments (Fig. 2*A*). To determine the appropriate period of acclimation for VSA and to assess the role of environmental stress induced by repeated VSAs, control mice were housed daily in VSA cages over the course of 12 days. These experiments indicated that mice with repeated daily VSA assessments maintained normal voiding patterns and that 1 day of exposure to the VSA cage was sufficient for acclimation (Supplemental Fig. S3). Mice exposed to CYP displayed significant changes in micturition patterns (Fig. 2*B*). CYP-exposed animals voided with small volume corner voiding and de novo edge voiding (Fig. 2*B*). The greatest changes in micturition patterns occurred early after CYP exposure (2–6 h) and were associated with an ~10-fold increase in the number of voids compared with vehicle-treated control animals (Fig. 2*B*). At 2–6 h, CYP-exposed animals voided a mean volume of 202 μL compared with 87 μL in controls (2.3-fold difference), and at 24–28 h, CYP-exposed animals voided a mean of 69 μL compared with 9 μL in controls (7.3-fold difference), which was not significantly different from later time points. In summary, we established a reproducible model of CYP-induced bladder injury and urinary dysfunction with multiple measurable end points to investigate the effects of pharmacological HIF activation on the prevention and therapy of CYP-associated bladder injury.

DMOG Protects Against CYP-Mediated Bladder Injury and Urinary Dysfunction

We next investigated the effects of DMOG-induced HIF activation in CYP-associated bladder injury and voiding dysfunction. DMOG is a small structural analog of 2-oxoglutarate and inhibits HIF-α degradation by competitively replacing 2-oxoglutarate from the PHD catalytic center (19, 34). In dose escalation experiments, we established that 16 mg DMOG delivered as a single intraperitoneal injection following CYP administration provided significant cytoprotection. To assess systemic responses to DMOG administration, we measured serum EPO levels, as DMOG is known to stimulate *Epo* transcription in the kidney and liver (20). We observed a 3.4-fold increase in serum EPO levels 6 h following DMOG administration and a concomitant increase in HIF target gene expression in whole bladder extracts (Fig. 3). Immunohistochemistry of paraffin-embedded bladder sections harvested 2 h after DMOG administration alone demonstrated HIF-1α-positive nuclei in the urothelium (Supplemental Fig. S4*A*). However, changes in transcript levels for HIF targets glucose transporter 1 (*Glut1*), VEGFA (*Vegfa*), and phosphoglycerate kinase 1 (*Pgk1*) in whole bladder extracts obtained from DMOG-treated mice at this time point were not detected (Fig. 3). Finally, immunohistochemistry of paraffin-embedded sections from bladders harvested 2 h after treatment with vehicle, CYP, or CYP in conjunction with DMOG, respectively, demonstrated HIF-1α-positive nuclei in the urothelium (Supplemental Fig. S5).

We assessed the effects of DMOG administration on CYP-induced bladder injury and urinary dysfunction using the experimental protocol shown in Fig. 4*A*. Administration of DMOG significantly improved bladder morphology in CYP-treated mice at 48 h after CYP exposure (Fig. 4*A*). Bladder weights were significantly reduced by approximately twofold in DMOG-treated animals compared with vehicle controls (Fig. 4*A*). Furthermore, DMOG treatment resulted in an approximately fourfold lower edema score and an approximately fivefold higher urothelial integrity score compared with vehicle controls and protected bladder permeability (Fig. 4*A* and Supplemental Fig. S1*B*). Immunohistochemistry for K_i-67 was performed to assess urothelial proliferation following CYP administration with or without DMOG. Forty-eight hours after CYP administration, urothelial proliferation was significantly reduced in the DMOG-treated group compared with vehicle-treated group (Supplemental Fig. S6). Micturition analysis revealed improvement in bladder function in DMOG-treated mice. Urinary frequency was significantly reduced by 9.2-fold at 2–6 h and by 7.8-fold at 24–28 h after CYP compared with vehicle-treated mice (Fig. 4*B*).

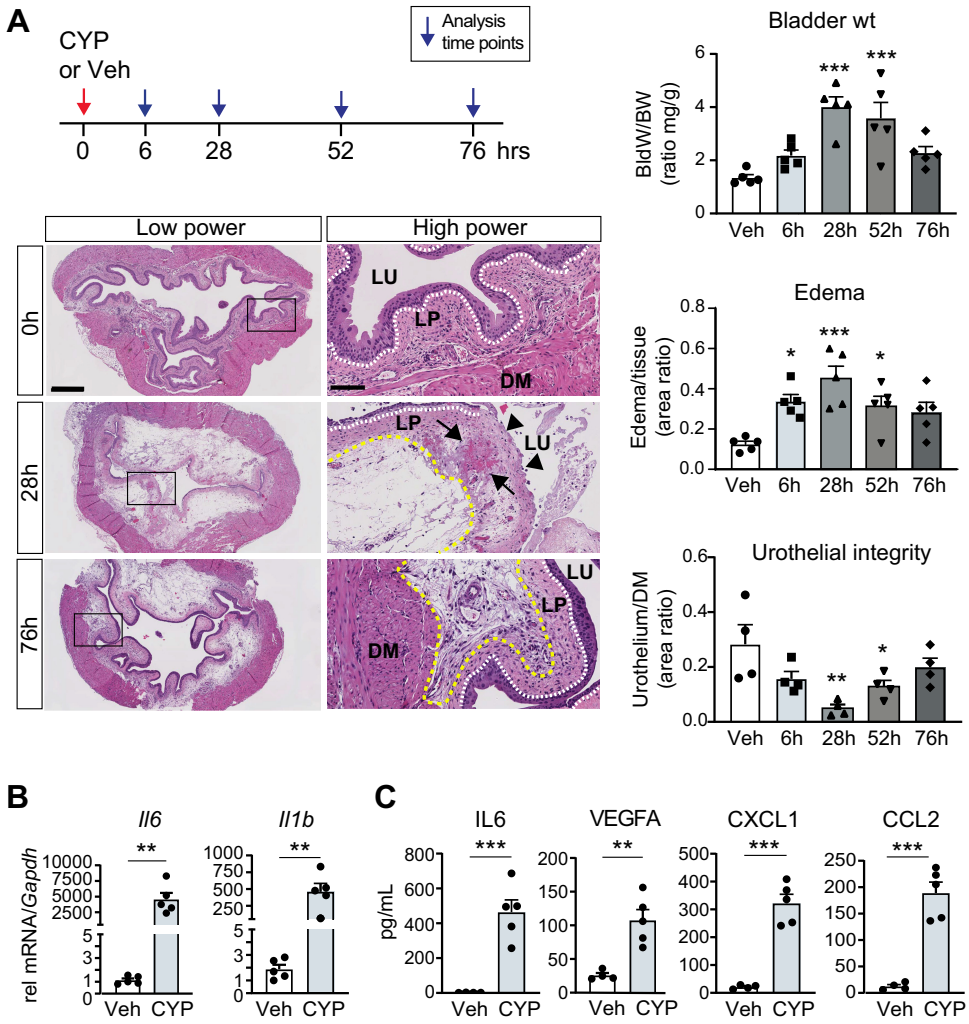

Figure 1. Cyclophosphamide (CYP) induces rapid bladder injury. *A*, *top*: schematic indicating the time points of analysis following a single injection of 300 mg/kg CYP in adult male mice (n = 5 per time point). *A*, *bottom left*: representative images of bladder sections stained with hematoxylin and eosin at 0 (baseline), 28, and 76 h following CYP administration. Low-power images demonstrate changes in overall morphology, urothelial sloughing, and transmural edema. Scale bar = 500 μm. Bladder hemorrhage is depicted by arrows, edema by yellow dashed lines, and urothelial sloughing by black arrowheads; the urothelial cell layer is lined by white dashed lines. *A*, *bottom right*: mean changes in the bladder-to-body weight ratio (Bld/BW), edema scores, and urothelial integrity scores (Urothelium/DM) over time. *B*: relative transcript levels of the inflammatory genes interleukin-6 (*Il6*) and interleukin-1b (*Il1b*) 6 h after CYP administration (n = 5 mice each). *C*: tissue cytokine levels (n = 5 mice each) for IL-6, vascular endothelial growth factor A (VEGFA), keratinocyte-derived chemokine/chemokine (C-X-C motif) ligand 1 (CXCL1), and monocyte chemoattractant protein-1/chemokine (C-C motif) ligand 2 (CCL2). Bars represent means ± SE. One-way ANOVA followed by Dunnett's post hoc analysis was used for the data sets shown in *A* and an unpaired Student's t test for the data sets shown in *B* and *C*. $^*P < 0.05$, $^{**}P < 0.01$, and $^{***}P < 0.001$. DM, detrusor muscle; LP, lamina propria; LU, bladder lumen; Veh, vehicle.

Consistent with the morphological and functional improvements was the reduction in bladder cytokine levels 6 h after CYP. We found a 1.7-fold reduction in IL-6, 1.2-fold reduction in IL-1b, 2-fold reduction in KC/CXCL1, 5.6-fold reduction in MCP-1/CCL2, and 1.5-fold reduction in MIP-2/CXCL2 (Fig. 4*C*). Taken together, our data indicate that DMOG treatment afforded significant cytoprotection from CYP-associated bladder injury and urinary dysfunction.

To address the possibility that the close timing of intraperitoneal DMOG and CYP administration might have interfered with CYP pharmacokinetics or metabolism potentially affecting the degree by which the bladder was exposed to acrolein, we measured urine 3-HPMA. 3-HPMA is a surrogate metabolite for acrolein, a reactive aldehyde that causes bladder injury in CYP-treated subjects (35, 36). Due to its high chemical reactivity, reliable MS-based measurements of urine acrolein levels were not feasible. For measurements of 3-HPMA levels, we collected and pooled hourly urine samples over the first 6 h after CYP exposure and found that urine 3-HPMA levels increased proportionally with CYP dosing, whereas 3-HPMA was not detectable in the urine from control mice without CYP exposure (Supplemental Fig. S7*A*). Urine 3-HPMA levels in mice exposed to 300 mg/kg CYP and treated with either DMOG or vehicle were not different (Supplemental Fig. S7*B*), whereas bladder weight in CYP/DMOG-treated mice was reduced by 1.7-fold compared with CYP/vehicle-treated mice, indicating cytoprotection despite the presence of high levels of urine 3-HPMA. These data suggest that the close timing of intraperitoneal DMOG and CYP administration did not significantly affect 3-HPMA levels in the bladder. To further address any potential for CYP and DMOG interaction, we collected blood samples at 0.5, 1, 2, and 4 h, respectively, from mice treated with CYP/vehicle or CYP/DMOG (Supplemental Fig. S8). Plasma CYP and 4-OH-CYP levels measured by MS showed no suppression of CYP or 4-OH-CYP levels by DMOG at any time point. Instead, we observed significantly higher levels of CYP at 0.5 and 1 h and then subsequently increased levels of 4-OH-CYP at 1 and 2 h. Taken together, these data suggested that no appreciable suppression of urine 3-HPMA and plasma CYP levels occurred with coadministration of DMOG and CYP by intraperitoneal injection.

Pretreatment With Molidustat Affords Cytoprotection and Maintains Normal Micturition Patterns

To corroborate the cytoprotective effects of pharmacological HIF stabilization in CYP-induced bladder injury and urinary dysfunction, we next investigated a more specific inhibitor of HIF-prolyl hydroxylation. We chose molidustat because it has good oral bioavailability and specificity for PHDs, as its affinity

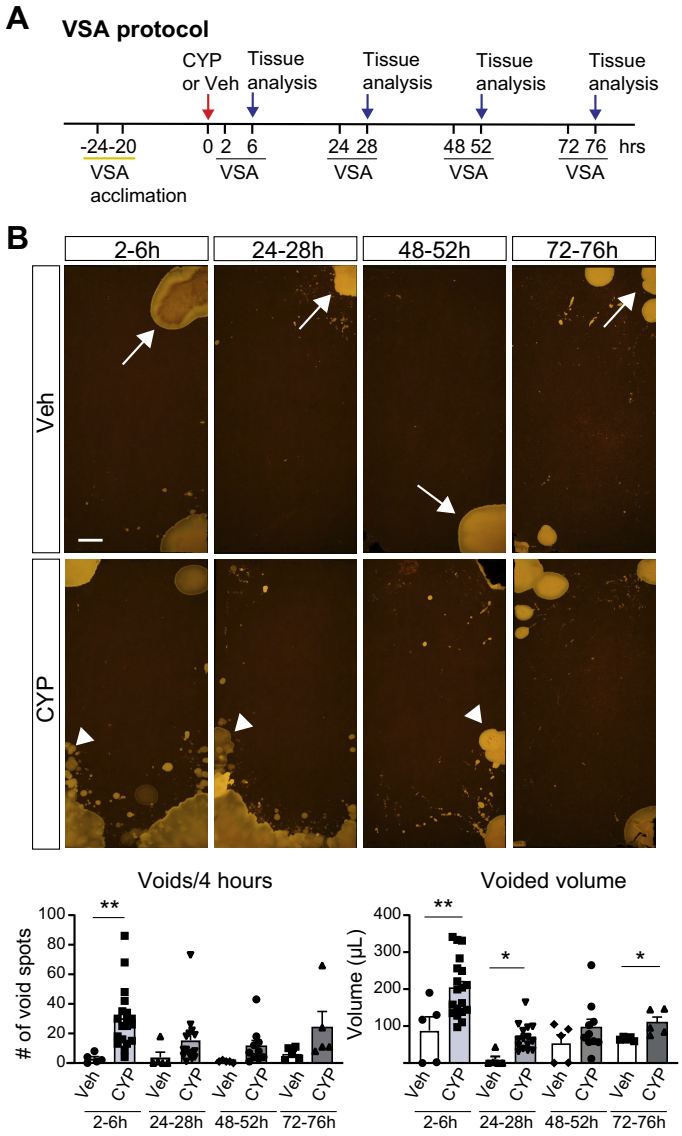

Figure 2. Cyclophosphamide (CYP) alters voiding patterns in mice. *A*: schematic detailing the timing of the 4-h void spot assay (VSA) in male mice following the administration of 300 mg/kg CYP. VSA analysis time points are indicated in relation to CYP administration. *B*: representative images of VSAs in vehicle (Veh)- and CYP-treated mice. Scale bar = 2.5 cm. Arrows indicate corner voiding. Arrowheads indicate small volume de novo edge voiding following CYP administration. Graphs depict the number of void spots at each time point and mean urine volume (in μL) for Veh-treated (n = 5) and CYP-treated mice (6 h: n = 20, 28 h: n = 15, 52 h: n = 10, and 76 h: n = 5). Bars represent means ± SE. An unpaired Student's t test was performed. *$P < 0.05$ and **$P < 0.01$.

for other 2-oxoglutarate dioxygenases is very low (23). Molidustat treatment produced a significant elevation in serum EPO levels 6 h after oral administration (Fig. 5*A*) and resulted in HIF-1α stabilization in urothelial and renal epithelial cells 2 h after oral administration (Supplemental Fig. S4). Significant changes in *Glut1*, *Vegfa*, and *Pgk1* transcript levels were not detected in whole bladder or kidney extracts, whereas renal *Epo* transcript levels increased by approximately fivefold (Supplemental Fig. S4).

We chose to administer three doses of molidustat (10 mg/kg) orally at 48, 24, and 6 h before treatment with CYP (Fig. 5*B*). In mice exposed to CYP, molidustat preserved bladder morphology, reduced edema, hemorrhage, and urothelial sloughing (Fig. 5*C*). By 48 h after CYP exposure, bladder weight was reduced by 1.6-fold, edema was reduced by 2.1-fold, and the urothelial integrity score was improved by 2.4-fold compared with vehicle-treated mice. Furthermore, like DMOG, molidustat restored micturition patterns in mice treated with CYP. In contrast to the numerous small volume corner and edge voids in mice that received CYP and vehicle, molidustat-treated animals maintained large volume corner voids characteristic of healthy mice (Fig. 5*D*). Regarding urinary frequency, the number of post-CYP voids was reduced by 2.8-fold at 2–6 h and by 2.3-fold at 24–28 h (Fig. 5*D*). Taken together, our data suggest that pretreatment with molidustat afforded significant protection against CYP-induced bladder injury and urinary dysfunction.

DISCUSSION

Here, we used a pharmacological approach to investigate the role of the HIF-PHD axis in inflammatory bladder injury and urinary dysfunction due to blood-urine barrier disruption. We used a murine model of CYP-induced bladder injury and investigated two small-molecule inhibitors of HIF-prolyl hydroxylation: DMOG and molidustat. Intraperitoneal DMOG administration or pretreatment with oral molidustat prevented the damaging effects of CYP as evidenced by preservation of normal bladder morphology and urothelial integrity, reduction in bladder cytokine levels, and maintenance of normal voiding patterns.

CYP-induced disruption of the blood-urine barrier in mice is a clinically relevant and frequently used model in experimental urology to study bladder inflammation, urothelial stress responses and regeneration, and detrusor muscle function (37–41). CYP is converted in the liver to 4-hydroxycyclophosphamide and then further metabolized to the cytotoxic intermediates phosphoramide mustard and acrolein, a small corrosive and reactive aldehyde, which is freely filtered by the kidneys and causes hemorrhagic cystitis (32). Depending on its concentration in the urine, acrolein causes variable degrees of urothelial injury (32). In patients receiving chemotherapy with CYP, acrolein exposure can lead to severe bladder injury in which mucosal ulcerations are associated with a spectrum of lower urinary tract issues including bladder pain, bleeding, tissue damage, and, in some cases, the need for cystectomy (4). The available treatment strategies primarily include hydration with intravenous fluids and administration of MESNA, an acrolein-binding compound (4). Yet, these interventions alone are not effective in all patients, and, as such, alternative therapies are needed for the prevention of CYP-associated bladder injury (42, 43).

We used two inhibitors of HIF-prolyl hydroxylation for our experiments: DMOG and molidustat. DMOG is a widely used experimental HIF stabilizer (19–22, 34), whereas molidustat is a new oral HIF-activating compound approved for the treatment of anemia of chronic kidney disease in Japan (25). A significant advantage of molidustat over DMOG is its excellent oral bioavailability and high affinity and specificity for PHD dioxygenases (23, 44). Like DMOG, molidustat afforded significant cytoprotection from CYP-induced bladder injury, providing strong support for the notion that the cytoprotective

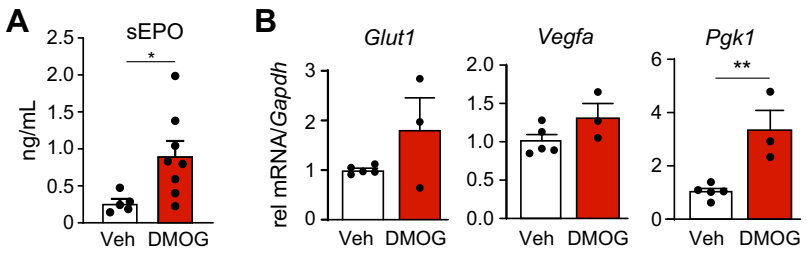

Figure 3. Dimethyloxalylglycine (DMOG) administration induces systemic and bladder hypoxia-inducible factor (HIF) responses. *A*: serum erythropoietin (sEPO) response to DMOG administration at 6 h (n = 8) compared with vehicle (Veh)-treated control mice (n = 5). *B*: HIF target gene expression in whole bladder tissue extracts (Veh: n = 5 and DMOG: n = 3). Transcript levels of glucose transporter 1 (*Glut1*), vascular endothelial growth factor A (*Vegfa*), and phosphoglycerate kinase 1 (*Pgk1*) were determined 6 h after single-dose DMOG administration. Bars represent means ± SE. An unpaired Student's t test was performed. $^{*}P < 0.05$ and $^{**}P < 0.01$.

effects observed in our study represented a drug class effect and resulted from the activation or modulation of HIF signaling.

Knowledge about the role of the HIF-PHD axis in bladder injury is limited and preclinical studies have produced conflicting results. Studies in a rat model of partial bladder outlet obstruction have suggested that both activation and inhibition of HIF signaling are beneficial. Treatment with the HIF-activating compound pyridine-2,4-dicarboxylate reduced bladder fibrosis and improved voiding function (45), whereas administration of the HIF-inhibiting compound 17-dimethylaminoethylamino-17-demethoxygeldanamycin also mitigated bladder injury (46, 47). Despite the limited data in the context of bladder injury, activation of

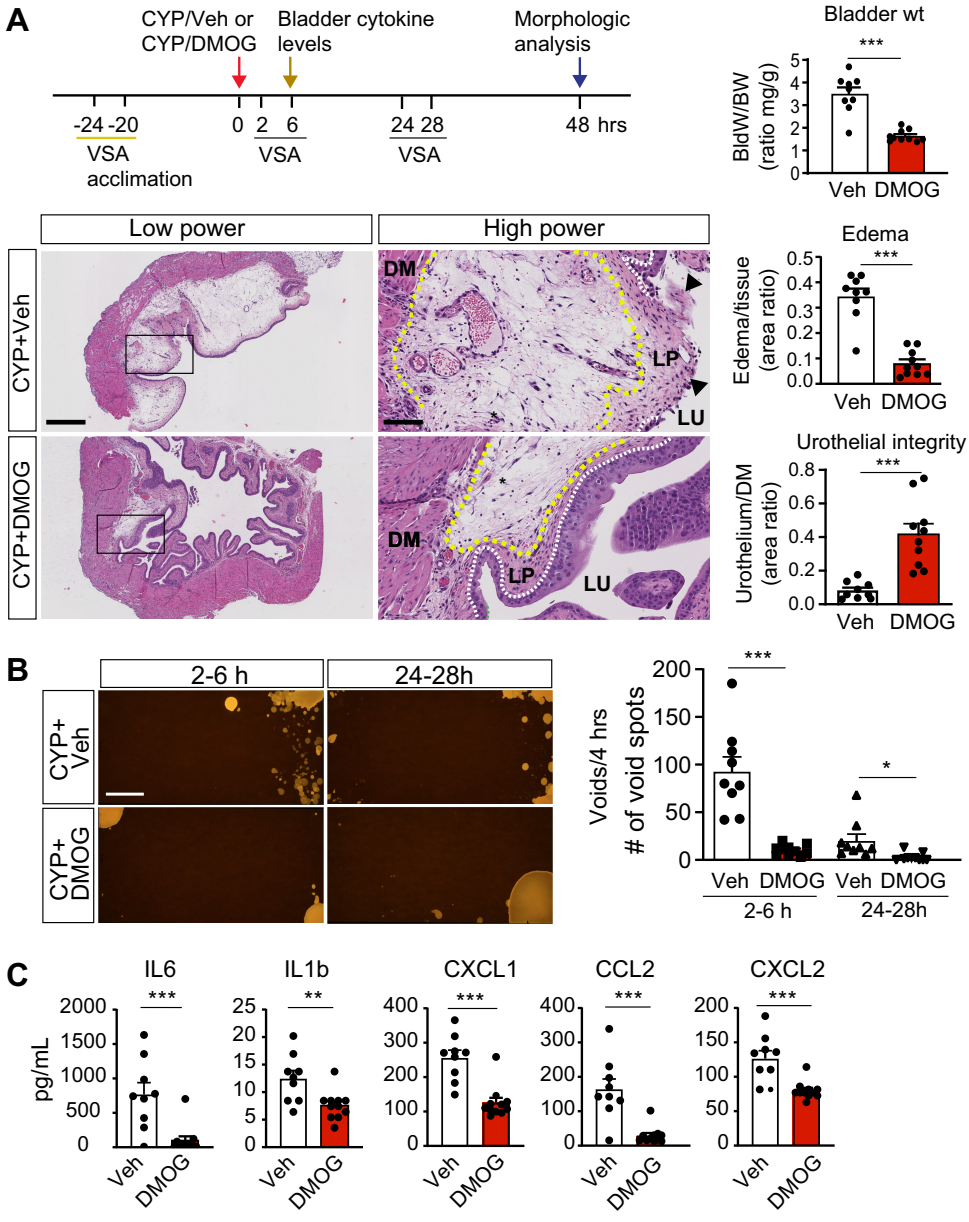

Figure 4. Dimethyloxalylglycine (DMOG) protects bladder integrity and voiding patterns in cyclophosphamide (CYP)-treated mice. *A*, *top*: schematic of the experimental protocol depicting dosing of DMOG in relation to CYP exposure and void spot analysis (VSA). *A*, *bottom left*: representative images of bladder sections stained with hematoxylin and eosin 48 h following CYP exposure. CYP administration was followed by either vehicle (Veh) or DMOG injection. Bladder wall edema is depicted by yellow dashed lines, urothelial sloughing by black arrowheads, and the urothelium by white dashed lines. Scale bars = 500 µm for low-power magnification and 100 µm for high-power magnification. *A*, *bottom right*: mean bladder-to-body weight ratios (BldW/BW), edema scores, and urothelial integrity scores (Urothelium/DM) at 48 h following CYP treatment. *B*, *left*: representative images of 4-h VSAs with normal corner voiding in DMOG-treated animals and small volume voids in Veh-treated animals. Scale bar = 5 cm. *B*, *right*: number of void spots at 2–6 and 24–28 h after CYP administration. *C*: bladder tissue cytokine levels 6 h after CYP exposure with or without DMOG [interleukin-6 (IL6), interleukin-1b (IL1b), keratinocyte-derived chemokine/chemokine (C-X-C motif) ligand 1 (CXCL1), monocyte chemoattractant protein-1/chemokine (C-C motif) ligand 2 (CCL2), and macrophage inflammatory protein-2/chemokine (C-X-C motif) ligand 2 (CXCL2)]. Bars represent means ± SE. An unpaired Student's t test was performed. $^{*}P < 0.05$, $^{**}P < 0.01$, and $^{***}P < 0.001$. DM, detrusor muscle, LP, lamina propria; LU, bladder lumen.

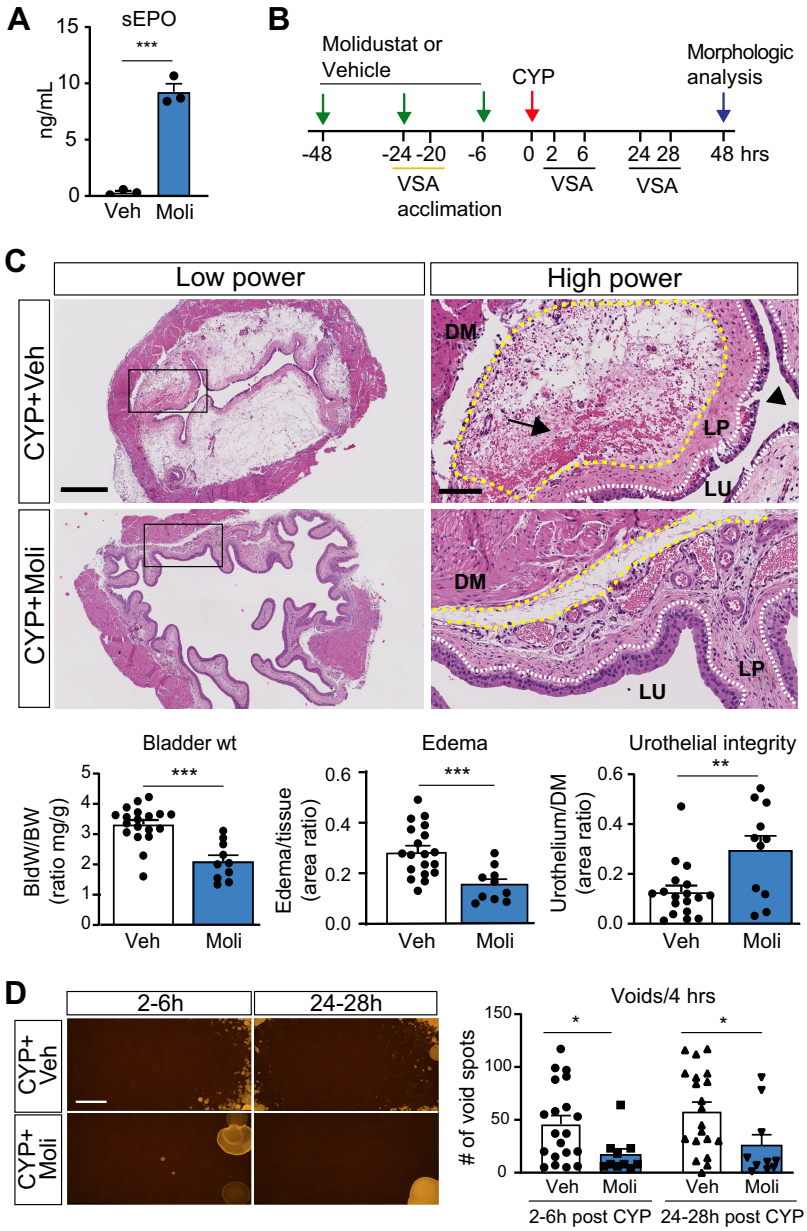

Figure 5. Molidustat (Moli) protects from cyclophosphamide (CYP)-induced bladder injury. *A*: serum erythropoietin (sEPO) levels 6 h after single-dose molidustat administration compared with vehicle (Veh)-treated controls (n = 3 each). *B*: schematic of the experimental protocol. The timing of Moli administration in relation to CYP treatment and void spot assays (VSAs) is shown. *C*: representative images of bladder sections stained with hematoxylin and eosin 48 h after CYP administration. Scale bars = 500 μm for low-power magnification and 100 μm for high-power magnification. Bladder hemorrhage is indicated by arrows, edema by yellow dashed lines, and urothelial sloughing by blackarrow heads. The urothelium is indicated by white dashed lines. Also shown are changes in the bladder weight-to-body weight ratio (BldW/BW), edema, and urothelial integrity scores at 48 h after CYP treatment in Veh- and Moli-treated cohorts [n = 10 for Moli (10 mg/kg) and n = 20 for Veh]. *D*, *left*: representative images of 4-h VSAs. Scale bar = 5 cm. *B*, *right*: number of void spots at the 2- to 6-h time point and 24- to 28-h time point after CYP administration in Veh-treated and Moli-treated cohorts. Bars represent means ± SE. An unpaired Student's t test was performed. $^*P < 0.05$, $^{**}P < 0.01$, and $^{***}P < 0.001$. DM, detrusor muscle; LP, lamina propria; LU, bladder lumen.

HIF signaling in other organs has been shown to afford significant protection from mucosal injury and inflammation. Treatment with DMOG or genetic PHD inactivation in intestinal epithelial cells improved survival following lethal doses of total abdominal or total body irradiation (22). Data from preclinical models of inflammatory bowel disease also demonstrated that targeted activation of the HIF pathway, either genetically or via pharmacological inhibition of HIF-prolyl hydroxylation, reduced inflammation, and improved barrier function (11, 21, 48, 49). Likewise, in models of experimental lung injury, acute HIF activation with DMOG resulted in better survival, which was associated with improved barrier function, reduced reactive oxygen species production, and reduced apoptosis (15, 50).

Loss of the urothelial barrier, which is the tightest and most impermeable mucosal barrier in the body, is likely to be the critical initiating step in the pathogenesis of CYP-induced bladder injury. Umbrella cells are the first cells to become injured in CYP-treated mice, and loss of the urothelial barrier exposes the underlying intermediate and basal urothelial cells to acrolein, thus promoting further damage and inflammation by stimulating innate immune responses (51). Enhancement of epithelial barrier function appears to be a key mechanism by which HIF promotes wound healing (52) or protects against chemically induced colitis in the gastrointestinal tract (11). In the intestine, HIF-1 increases the expression of intestinal trefoil factors (11, 53), which strengthens the mucosal barrier and protects from inflammation, making the HIF-PHD axis an excellent therapeutic target for the prevention and treatment of inflammatory bowel disease (8).

In our study, pharmacological HIF activation resulted in a substantial suppression of cytokine expression in the bladder. Likewise, suppression of the expression of proinflammatory cytokines, such as IL-1b, IL-6, and TNF-α, with immune-

AJP-Renal Physiol • doi:10.1152/ajprenal.00344.2021 • www.ajprenal.org

modulatory protein IPSE (IL-4-inducing principle from Schistosoma eggs) ameliorated ifosfamide-induced hemorrhagic cystitis (42). It is therefore plausible that HIF-mediated cytokine suppression may have contributed to the beneficial effects of HIF-prolyl hydroxylation inhibition in CYP-induced bladder injury. It is well established that the HIF-PHD axis plays a critical role in the regulation of innate and humoral immune responses in part through interdependence with NF-κB signaling, which is highly cell type and context-dependent (54, 55). Consistent with our observations are findings in a rat model of inflammatory anemia, where molidustat suppressed MCP-1/CCL2 expression in the kidney (44). MCP-1/CCL2 is a chemoattractant for monocytes and mast cells and has disease-promoting activity in chronic cystitis by facilitating mast cell degranulation (56). Furthermore, MCP-1/CCL2 has been implicated in the regulation of micturition reflexes in rats, as inhibition of MCP-1/CCL2 signaling reduced void frequency after CYP exposure (57).

Our study is not without limitations. The present work does not delineate and/or validate underpinning mechanisms that drive HIF-PHI-mediated cytoprotection in the bladder. Furthermore, we have shown that CYP exposure alone stabilizes HIF-1α in the bladder urothelium. From our experiments, we were unable to determine to what degree HIF responses in CYP-injured bladders were modulated or augmented by pharmacological PHD inhibition and to what degree bladder protection afforded by systemic HIF-PHI administration involved bladder intrinsic responses or remote effects, as previously shown for other organs (58, 59). A precise understanding of these mechanisms will be crucial for the development of HIF-PHIs as a potential preclinical lead in bladder injury. This would include the use of genetic models to identify the cell types that mediate protective effects in the bladder. Although our study clearly demonstrates that pharmacological HIF activation is cytoprotective when HIF-PHIs are administered before CYP-induced bladder injury, they did not investigate the effects of HIF-PHI administration on established bladder injury. This will be an area for future study and of great clinical relevance as many patients present after the onset of injury.

Perspectives and Significance

In summary, our data demonstrate that pharmacological inhibition of PHDs is protective in acute CYP-induced bladder injury. The implications of our work highlight the therapeutic potential of HIF-prolyl hydroxylase inhibition not only for the prevention and treatment of inflammatory bladder injury induced by CYP exposure but also for patients with other forms of cystitis due to blood-urine barrier disruption. Although the mechanisms by which activation of the HIF-PHD axis protects from bladder injury are not clear and most likely involve multiple signaling pathways and cell types, our study provides a strong basis for future detailed mechanistic investigations. If such future endeavors are successful, HIF-PHI treatment would be a new clinically relevant therapeutic lead for patients with cystitis.

SUPPLEMENTAL DATA

Supplemental Table S1 and Supplemental Figs. S1–S8: https://doi.org/10.6084/m9.figshare.16574267.v1.

GRANTS

This work was supported by funds from the Department of Urology (to D.B.C.); Division of Pediatric Urology (to D.B.C.); the John W. Brock III Pediatric Urology Research and Education fund (to D.B.C.); National Institutes of Health (NIH) Grants K08DK106472 (to D.B.C.), R01DK101791 (to V.H.H.), and R01DK081646 (to V.H.H.); and the Krick-Brooks Chair in Nephrology at Vanderbilt University (to V.H.H.). We acknowledge support by the Vanderbilt O'Brien Kidney Center (NIH Grant P30DK114809) and the Vanderbilt University Medical Center Translational Pathology Shared Resource for the help with tissue processing (NIH Grant P30CA068485) as well as the Vanderbilt Mouse Metabolic Phenotyping Center (NIH Grant DK059637) and the Vanderbilt University Diabetes Research and Training Center (NIH Grant P30DK020593). Whole slide imaging was performed in the Digital Histology Shared Resource at Vanderbilt University Medical Center (https://www.vumc.org/dhsr/welcome). Information about work performed in the Haase laboratory can be found at https://www.haaselab.org.

DISCLOSURES

No conflicts of interest, financial or otherwise, are declared by the authors.

AUTHOR CONTRIBUTIONS

D.B.C. and V.H.H. conceived and designed research; D.B.C., C.M.C.T., B.L., A.S.T., S.D., M.D.M., A.G.D., O.D., H.K., and V.H.H. performed experiments; D.B.C., C.M.C.T., B.L., A.S.T., S.D., M.D.M., A.G.D., O.D., H.K., and V.H.H. analyzed data; D.B.C., C.M.C.T., B.L., S.D., O.D., H.K., and V.H.H. interpreted results of experiments; D.B.C., H.K., and V.H.H. prepared figures; D.B.C. and V.H.H. drafted the manuscript; D.B.C., H.K., and V.H.H. edited and revised the manuscript; D.B.C., C.M.C.T., B.L., A.S.T., S.D., M.D.M, A.G.D., O.D., H.K., and V.H.H. approved the final version of manuscript.

REFERENCES

1. **Freedman AL**; **Urologic Diseases in America Project.** Urologic Diseases in North America Project: trends in resource utilization for urinary tract infections in children. *J Urol* 173: 949–954, 2005. doi:10.1097/01.ju.0000152092.03931.9a.
2. **Griebling TL.** Urologic Diseases in America Project: trends in resource use for urinary tract infections in men. *J Urol* 173: 1288–1294, 2005. doi:10.1097/01.ju.0000155595.98120.8e.
3. **Griebling TL.** Urologic Diseases in America Project: trends in resource use for urinary tract infections in women. *J Urol* 173: 1281–1287, 2005. doi:10.1097/01.ju.0000155596.98780.82.
4. **Matz EL**, **Hsieh MH.** Review of advances in uroprotective agents for cyclophosphamide- and ifosfamide-induced hemorrhagic cystitis. *Urology* 100: 16–19, 2017. doi:10.1016/j.urology.2016.07.030.
5. **Zwaans BM**, **Chancellor MB**, **Lamb LE.** Modeling and treatment of radiation cystitis. *Urology* 88: 14–21, 2016. doi:10.1016/j.urology.2015.11.001.
6. **Stephany HA**, **Strand DW**, **Ching CB**, **Tanaka ST**, **Milne GL**, **Cajaiba MM**, **Thomas JC**, **Pope JC 4th**, **Adams MC**, **Brock JW 3rd**, **Hayward SW**, **Matusik RJ**, **Clayton DB.** Chronic cyclic bladder over distention up-regulates hypoxia dependent pathways. *J Urol* 190: 1603–1609, 2013. doi:10.1016/j.juro.2013.02.026.
7. **Ito S**, **Nomura T**, **Ueda T**, **Inui S**, **Morioka Y**, **Honjo H**, **Fukui A**, **Fujihara A**, **Hongo F**, **Ukimura O.** Gene expression profiles during tissue remodeling following bladder outlet obstruction. *Sci Rep* 11: 13171, 2021. doi:10.1038/s41598-021-92756-1.
8. **Colgan SP.** Targeting hypoxia in inflammatory bowel disease. *J Investig Med* 64: 364–368, 2016. doi:10.1097/JIM.0000000000000218.

9. **Eltzschig HK**, **Bratton DL**, **Colgan SP.** Targeting hypoxia signalling for the treatment of ischaemic and inflammatory diseases. *Nat Rev Drug Discov* 13: 852–869, 2014. doi:10.1038/nrd4422.
10. **Semenza GL.** Pharmacologic targeting of hypoxia-inducible factors. *Annu Rev Pharmacol Toxicol* 59: 379–403, 2019. doi:10.1146/annurev-pharmtox-010818-021637.
11. **Karhausen J**, **Furuta GT**, **Tomaszewski JE**, **Johnson RS**, **Colgan SP**, **Haase VH.** Epithelial hypoxia-inducible factor-1 is protective in murine experimental colitis. *J Clin Invest* 114: 1098–1106, 2004. doi:10.1172/JCI21086.
12. **McIntosh BE**, **Hogenesch JB**, **Bradfield CA.** Mammalian Per-Arnt-Sim proteins in environmental adaptation. *Annu Rev Physiol* 72: 625–645, 2010. doi:10.1146/annurev-physiol-021909-135922.
13. **Loenarz C**, **Schofield CJ.** Expanding chemical biology of 2-oxoglutarate oxygenases. *Nat Chem Biol* 4: 152–156, 2008. doi:10.1038/nchembio0308-152.
14. **Kaelin WG Jr**, **Ratcliffe PJ.** Oxygen sensing by metazoans: the central role of the HIF hydroxylase pathway. *Mol Cell* 30: 393–402, 2008. doi:10.1016/j.molcel.2008.04.009.
15. **Eltzschig HK**, **Eckle T.** Ischemia and reperfusion—from mechanism to translation. *Nat Med* 17: 1391–1401, 2011. doi:10.1038/nm.2507.
16. **Kapitsinou PP**, **Haase VH.** Molecular mechanisms of ischemic preconditioning in the kidney. *Am J Physiol Renal Physiol* 309: F821–F834, 2015. doi:10.1152/ajprenal.00224.2015.
17. **Chan MC**, **Holt-Martyn JP**, **Schofield CJ**, **Ratcliffe PJ.** Pharmacological targeting of the HIF hydroxylases—a new field in medicine development. *Mol Aspects Med* 47–48: 54–75, 2016. doi:10.1016/j.mam.2016.01.001.
18. **Schofield CJ**, **Ratcliffe PJ.** Oxygen sensing by HIF hydroxylases. *Nat Rev Mol Cell Biol* 5: 343–354, 2004. doi:10.1038/nrm1366.
19. **Jaakkola P**, **Mole DR**, **Tian YM**, **Wilson MI**, **Gielbert J**, **Gaskell SJ**, **von Kriegsheim A**, **Hebestreit HF**, **Mukherji M**, **Schofield CJ**, **Maxwell PH**, **Pugh CW**, **Ratcliffe PJ.** Targeting of HIF-α to the von Hippel-Lindau ubiquitylation complex by O_2-regulated prolyl hydroxylation. *Science* 292: 468–472, 2001. doi:10.1126/science.1059796.
20. **Rankin EB**, **Biju MP**, **Liu Q**, **Unger TL**, **Rha J**, **Johnson RS**, **Simon MC**, **Keith B**, **Haase VH.** Hypoxia-inducible factor-2 (HIF-2) regulates hepatic erythropoietin in vivo. *J Clin Invest* 117: 1068–1077, 2007. doi:10.1172/JCI30117.
21. **Cummins EP**, **Seeballuck F**, **Keely SJ**, **Mangan NE**, **Callanan JJ**, **Fallon PG**, **Taylor CT.** The hydroxylase inhibitor dimethyloxalylglycine is protective in a murine model of colitis. *Gastroenterology* 134: 156–165, 2008. doi:10.1053/j.gastro.2007.10.012.
22. **Taniguchi CM**, **Miao YR**, **Diep AN**, **Wu C**, **Rankin EB**, **Atwood TF**, **Xing L**, **Giaccia AJ.** PHD inhibition mitigates and protects against radiation-induced gastrointestinal toxicity via HIF2. *Sci Transl Med* 6: 236ra64, 2014. doi:10.1126/scitranslmed.3008523.
23. **Yeh TL**, **Leissing TM**, **Abboud MI**, **Thinnes CC**, **Atasoylu O**, **Holt-Martyn JP**, **Zhang D**, **Tumber A**, **Lippl K**, **Lohans CT**, **Leung IKH**, **Morcrette H**, **Clifton IJ**, **Claridge TDW**, **Kawamura A**, **Flashman E**, **Lu X**, **Ratcliffe PJ**, **Chowdhury R**, **Pugh CW**, **Schofield CJ.** Molecular and cellular mechanisms of HIF prolyl hydroxylase inhibitors in clinical trials. *Chem Sci* 8: 7651–7668, 2017. doi:10.1039/c7sc02103h.
24. **Beck H**, **Jeske M**, **Thede K**, **Stoll F**, **Flamme I**, **Akbaba M**, **Erguden JK**, **Karig G**, **Keldenich J**, **Oehme F**, **Militzer HC**, **Hartung IV**, **Thuss U.** Discovery of molidustat (BAY 85-3934): a small-molecule oral HIF-prolyl hydroxylase (HIF-PH) inhibitor for the treatment of renal anemia. *ChemMedChem* 13: 988–1003, 2018. doi:10.1002/cmdc.201700783.
25. **Haase VH.** Hypoxia-inducible factor-prolyl hydroxylase inhibitors in the treatment of anemia of chronic kidney disease. *Kidney Int Suppl* 11: 8–25, 2021. doi:10.1016/j.kisu.2020.12.002.
26. **Hill WG**, **Zeidel ML**, **Bjorling DE**, **Vezina CM.** Void spot assay: recommendations on the use of a simple micturition assay for mice. *Am J Physiol Renal Physiol* 315: F1422–F1429, 2018. doi:10.1152/ajprenal.00350.2018.
27. **Wegner KA**, **Abler LL**, **Oakes SR**, **Mehta GS**, **Ritter KE**, **Hill WG**, **Zwaans BM**, **Lamb LE**, **Wang Z**, **Bjorling DE**, **Ricke WA**, **Macoska J**, **Marker PC**, **Southard-Smith EM**, **Eliceiri KW**, **Vezina CM.** Void spot assay procedural optimization and software for rapid and objective quantification of rodent voiding function, including overlapping urine spots. *Am J Physiol Renal Physiol* 315: F1067–F1080, 2018. doi:10.1152/ajprenal.00245.2018.
28. **Hu P**, **Deng FM**, **Liang FX**, **Hu CM**, **Auerbach AB**, **Shapiro E**, **Wu XR**, **Kachar B**, **Sun TT.** Ablation of uroplakin III gene results in small urothelial plaques, urothelial leakage, and vesicoureteral reflux. *J Cell Biol* 151: 961–972, 2000. doi:10.1083/jcb.151.5.961.
29. **Kobayashi H**, **Liu J**, **Urrutia AA**, **Burmakin M**, **Ishii K**, **Rajan M**, **Davidoff O**, **Saifudeen Z**, **Haase VH.** Hypoxia-inducible factor prolyl-4-hydroxylation in FOXD1 lineage cells is essential for normal kidney development. *Kidney Int* 92: 1370–1383, 2017. doi:10.1016/j.kint.2017.06.015.
30. **Zheng L**, **Park J**, **Walls M**, **Tully M**, **Jannasch A**, **Cooper B**, **Shi R.** Determination of urine 3-HPMA, a stable acrolein metabolite in a rat model of spinal cord injury. *J Neurotrauma* 30: 1334–1341, 2013. doi:10.1089/neu.2013.2888.
31. **Carmella SG**, **Chen M**, **Zarth A**, **Hecht SS.** High throughput liquid chromatography-tandem mass spectrometry assay for mercapturic acids of acrolein and crotonaldehyde in cigarette smokers' urine. *J Chromatogr B Analyt Technol Biomed Life Sci* 935: 36–40, 2013. doi:10.1016/j.jchromb.2013.07.004.
32. **Ramirez DA**, **Collins KP**, **Aradi AE**, **Conger KA**, **Gustafson DL.** Kinetics of cyclophosphamide metabolism in humans, dogs, cats, and mice and relationship to cytotoxic activity and pharmacokinetics. *Drug Metab Dispos* 47: 257–268, 2019. [Erratum in *Drug Metab Dispos* 48: 63, 2020]. doi:10.1124/dmd.118.083766.
33. **Bhat N**, **Kalthur SG**, **Padmashali S**, **Monappa V.** Toxic effects of different doses of cyclophosphamide on liver and kidney tissue in Swiss albino mice: a histopathological study. *Ethiop J Health Sci* 28: 711–716, 2018. doi:10.4314/ejhs.v28i6.5.
34. **Epstein AC**, **Gleadle JM**, **McNeill LA**, **Hewitson KS**, **O'Rourke J**, **Mole DR**, **Mukherji M**, **Metzen E**, **Wilson MI**, **Dhanda A**, **Tian YM**, **Masson N**, **Hamilton DL**, **Jaakkola P**, **Barstead R**, **Hodgkin J**, **Maxwell PH**, **Pugh CW**, **Schofield CJ**, **Ratcliffe PJ.** *C. elegans* EGL-9 and mammalian homologs define a family of dioxygenases that regulate HIF by prolyl hydroxylation. *Cell* 107: 43–54, 2001. doi:10.1016/S0092-8674(01)00507-4.
35. **Cox PJ.** Cyclophosphamide cystitis—identification of acrolein as the causative agent. *Biochem Pharmacol* 28: 2045–2049, 1979. doi:10.1016/0006-2952(79)90222-3.
36. **Bjorling DE**, **Elkahwaji JE**, **Bushman W**, **Janda LM**, **Boldon K**, **Hopkins WJ**, **Wang ZY.** Acute acrolein-induced cystitis in mice. *BJU Int* 99: 1523–1529, 2007. doi:10.1111/j.1464-410X.2007.06773.x.
37. **Hughes FM Jr**, **Vivar NP**, **Kennis JG**, **Pratt-Thomas JD**, **Lowe DW**, **Shaner BE**, **Nietert PJ**, **Spruill LS**, **Purves JT.** Inflammasomes are important mediators of cyclophosphamide-induced bladder inflammation. *Am J Physiol Renal Physiol* 306: F299–F308, 2014. doi:10.1152/ajprenal.00297.2013.
38. **Gandhi D**, **Molotkov A**, **Batourina E**, **Schneider K**, **Dan H**, **Reiley M**, **Laufer E**, **Metzger D**, **Liang F**, **Liao Y**, **Sun TT**, **Aronow B**, **Rosen R**, **Mauney J**, **Adam R**, **Rosselot C**, **Van Batavia J**, **McMahon A**, **McMahon J**, **Guo JJ**, **Mendelsohn C.** Retinoid signaling in progenitors controls specification and regeneration of the urothelium. *Dev Cell* 26: 469–482, 2013. doi:10.1016/j.devcel.2013.07.017.
39. **Guo M**, **Chang P**, **Hauke E**, **Girard BM**, **Tooke K**, **Ojala J**, **Malley SM**, **Hsiang H**, **Vizzard MA.** Expression and function of chemokines CXCL9-11 in micturition pathways in cyclophosphamide (CYP)-induced cystitis and somatic sensitivity in mice. *Front Syst Neurosci* 12: 9, 2018. doi:10.3389/fnsys.2018.00009.
40. **Tooke K**, **Girard B**, **Vizzard MA.** Functional effects of blocking VEGF/VEGFR2 signaling in the rat urinary bladder in acute and chronic CYP-induced cystitis. *Am J Physiol Renal Physiol* 317: F43–F51, 2019. doi:10.1152/ajprenal.00083.2019.
41. **Juszczak K**, **Krolczyk G**, **Filipek M**, **Dobrowolski ZF**, **Thor PJ.** Animal models of overactive bladder: cyclophosphamide (CYP)-induced cystitis in rats. *Folia Med Cracov* 48: 113–123, 2007.
42. **Mbanefo EC**, **Le L**, **Zee R**, **Banskota N**, **Ishida K**, **Pennington LF**, **Odegaard JI**, **Jardetzky TS**, **Alouffi A**, **Falcone FH**, **Hsieh MH.** IPSE, a urogenital parasite-derived immunomodulatory protein, ameliorates ifosfamide-induced hemorrhagic cystitis through downregulation of pro-inflammatory pathways. *Sci Rep* 9: 1586, 2019. doi:10.1038/s41598-018-38274-z.
43. **Mbanefo EC**, **Le L**, **Pennington LF**, **Odegaard JI**, **Jardetzky TS**, **Alouffi A**, **Falcone FH**, **Hsieh MH.** Therapeutic exploitation of IPSE, a urogenital parasite-derived host modulatory protein, for chemotherapy-induced hemorrhagic cystitis. *FASEB J* 32: 4408–4419, 2018. doi:10.1096/fj.201701415R.

44. **Flamme I**, **Oehme F**, **Ellinghaus P**, **Jeske M**, **Keldenich J**, **Thuss U.** Mimicking hypoxia to treat anemia: HIF-stabilizer BAY 85-3934 (Molidustat) stimulates erythropoietin production without hypertensive effects. *PLoS One* 9: e111838, 2014. doi:10.1371/journal.pone.0111838.
45. **Chung JM**, **Jung MJ**, **Lee SJ**, **Lee SD.** Effects of prolyl 4-hydroxylase inhibitor on bladder function, bladder hypertrophy and collagen subtypes in a rat model with partial bladder outlet obstruction. *Urology* 80: 1390.e7-12, 2012. doi:10.1016/j.urology.2012.07.019.
46. **Iguchi N**, **Malykhina AP**, **Wilcox DT.** Inhibition of HIF reduces bladder hypertrophy and improves bladder function in murine model of partial bladder outlet obstruction. *J Urol* 195: 1250–1256, 2016. doi:10.1016/j.juro.2015.08.001.
47. **Iguchi N**, **Donmez MI**, **Malykhina AP**, **Carrasco A Jr**, **Wilcox DT.** Preventative effects of a HIF inhibitor, 17-DMAG, on partial bladder outlet obstruction-induced bladder dysfunction. *Am J Physiol Renal Physiol* 313: F1149–F1160, 2017. doi:10.1152/ajprenal.00240.2017.
48. **Tambuwala MM**, **Cummins EP**, **Lenihan CR**, **Kiss J**, **Stauch M**, **Scholz CC**, **Fraisl P**, **Lasitschka F**, **Mollenhauer M**, **Saunders SP**, **Maxwell PH**, **Carmeliet P**, **Fallon PG**, **Schneider M**, **Taylor CT.** Loss of prolyl hydroxylase-1 protects against colitis through reduced epithelial cell apoptosis and increased barrier function. *Gastroenterology* 139: 2093–2101, 2010. doi:10.1053/j.gastro.2010.06.068.
49. **Keely S**, **Campbell EL**, **Baird AW**, **Hansbro PM**, **Shalwitz RA**, **Kotsakis A**, **McNamee EN**, **Eltzschig HK**, **Kominsky DJ**, **Colgan SP.** Contribution of epithelial innate immunity to systemic protection afforded by prolyl hydroxylase inhibition in murine colitis. *Mucosal Immunol* 7: 114–123, 2014. doi:10.1038/mi.2013.29.
50. **Olson N**, **Hristova M**, **Heintz NH**, **Lounsbury KM**, **van der Vliet A.** Activation of hypoxia-inducible factor-1 protects airway epithelium against oxidant-induced barrier dysfunction. *Am J Physiol Lung Cell Mol Physiol* 301: L993–L1002, 2011. doi:10.1152/ajplung.00250.2011.
51. **Korkmaz A**, **Topal T**, **Oter S.** Pathophysiological aspects of cyclophosphamide and ifosfamide induced hemorrhagic cystitis; implication of reactive oxygen and nitrogen species as well as PARP activation. *Cell Biol Toxicol* 23: 303–312, 2007. doi:10.1007/s10565-006-0078-0.
52. **Rezvani HR**, **Ali N**, **Serrano-Sanchez M**, **Dubus P**, **Varon C**, **Ged C**, **Pain C**, **Cario-Andre M**, **Seneschal J**, **Taieb A**, **de Verneuil H**, **Mazurier F.** Loss of epidermal hypoxia-inducible factor-1alpha accelerates epidermal aging and affects re-epithelialization in human and mouse. *J Cell Sci* 124: 4172–4183, 2011. doi:10.1242/jcs.082370.
53. **Furuta GT**, **Turner JR**, **Taylor CT**, **Hershberg RM**, **Comerford K**, **Narravula S**, **Podolsky DK**, **Colgan SP.** Hypoxia-inducible factor 1-dependent induction of intestinal trefoil factor protects barrier function during hypoxia. *J Exp Med* 193: 1027–1034, 2001. doi:10.1084/jem.193.9.1027.
54. **Taylor CT**, **Doherty G**, **Fallon PG**, **Cummins EP.** Hypoxia-dependent regulation of inflammatory pathways in immune cells. *J Clin Invest* 126: 3716–3724, 2016. doi:10.1172/JCI84433.
55. **D'Ignazio L**, **Bandarra D**, **Rocha S.** NF-κB and HIF crosstalk in immune responses. *FEBS J* 283: 413–424, 2016. doi:10.1111/febs.13578.
56. **Bicer F**, **Altuntas CZ**, **Izgi K**, **Ozer A**, **Kavran M**, **Tuohy VK**, **Daneshgari F.** Chronic pelvic allodynia is mediated by CCL2 through mast cells in an experimental autoimmune cystitis model. *Am J Physiol Renal Physiol* 308: F103–F113, 2015. doi:10.1152/ajprenal.00202.2014.
57. **Arms L**, **Girard BM**, **Malley SE**, **Vizzard MA.** Expression and function of CCL2/CCR2 in rat micturition reflexes and somatic sensitivity with urinary bladder inflammation. *Am J Physiol Renal Physiol* 305: F111–F122, 2013. doi:10.1152/ajprenal.00139.2013.
58. **Hoppe G**, **Yoon S**, **Gopalan B**, **Savage AR**, **Brown R**, **Case K**, **Vasanji A**, **Chan ER**, **Silver RB**, **Sears JE.** Comparative systems pharmacology of HIF stabilization in the prevention of retinopathy of prematurity. *Proc Natl Acad Sci USA* 113: E2516–E2525, 2016. doi:10.1073/pnas.1523005113.
59. **Olenchock BA**, **Moslehi J**, **Baik AH**, **Davidson SM**, **Williams J**, **Gibson WJ**, **Chakraborty AA**, **Pierce KA**, **Miller CM**, **Hanse EA**, **Kelekar A**, **Sullivan LB**, **Wagers AJ**, **Clish CB**, **Vander Heiden MG**, **Kaelin WG Jr.** EGLN1 inhibition and rerouting of α-ketoglutarate suffice for remote ischemic protection. *Cell* 164: 884–895, 2016. [Erratum in *Cell* 165: 497, 2016]. doi:10.1016/j.cell.2016.02.006.